

NANO-INDENTATION INVESTIGATIONS OF THE MECHANICAL PROPERTIES OF THIN TiO₂, WO₃ AND THEIR COMPOSITES LAYERS, DEPOSITED BY SPRAY PYROLYSIS

PREISKAVE MEHANSKIH LASTNOSTI Z NANOTRDOTO TANKIH TiO₂, WO₃ IN NJUNIH KOMPOZITNIH PLASTI, NANEŠENIH S PRŠILNO PIROLIZO

Sabina Cherneva¹, Roumen Iankov¹, Nenad Radic², Bosko Grbic²,
Maria Datcheva¹, Dimitar Stoychev³

¹Bulgarian Academy of Sciences, Institute of Mechanics, Acad. G. Bonchev str., bl.4, 1113 Sofia, Bulgaria

²ChTM, University of Belgrade, Department of Catalysis and Chemical Engineering, Njegoseva 12, 11000 Belgrade, Serbia

³Bulgarian Academy of Sciences, Institute of Physical Chemistry, Acad. G. Bonchev str., bl.11,1113 Sofia, Bulgaria
stoychev@ipc.bas.bg

Prejem rokopisa – received: 2015-07-10; sprejem za objavo – accepted for publication: 2016-01-05

doi:10.17222/mit.2015.216

The aim of the present work is to determine the indentation hardness (H_{IT}) and indentation modulus (E_{IT}) of pure TiO₂ and WO₃ thin films, as well as thin films composed of different TiO₂ and WO₃ proportions and deposited by spray pyrolysis on a stainless-steel (OC 404) substrate. Since the H_{IT} and E_{IT} of the films are properties expected to depend on the phase-chemical composition, morphology, structure and their changes when increasing the WO₃ content in the TiO₂-WO₃ composite film, the correlation between the mechanical and structural properties is also addressed. The obtained results show that H_{IT} and E_{IT} strongly depend on the concentration of the co-deposited WO₃. The determined values of H_{IT} and E_{IT} noticeably decrease (in comparison with H_{IT} and E_{IT} of the pure (100 %) TiO₂ layer) when very low concentrations of WO₃ (up to 2.5 % of W) are co-deposited. At higher concentrations of the co-deposited WO₃ (more than 2.5 % of W), the H_{IT} and E_{IT} values increase almost linearly with an increase of the WO₃ in the precursor. The observed non-proportional behavior of H_{IT} and E_{IT} is associated with specific changes of the structure and a development of defects in the deposited TiO₂-WO₃ composite phase, as well as with the increase in the amount of the formed separate WO₃ phase (with increasing of WO₃ (H₂W₃O₁₂) in the working solution) surrounded by solitary TiO₂ particles.

Keywords: inorganic compounds, chemical synthesis, electron microscopy, elastic properties

Namen predstavljenega dela je določiti trdoto vtiska (H_{IT}) in modul vtiska (E_{IT}) v tankih filmih iz čistega TiO₂ in WO₃, kot tudi tankih filmov, sestavljenih iz različnih delov TiO₂ in WO₃, nanešenih s pršilno pirolizo na podlago iz nerjavnega jekla (OC 404). Ker se pričakuje, da sta lastnosti filma H_{IT} in E_{IT} odvisni od kemijske sestave faz, morfologije, strukture in njenih sprememb, ko povečujemo delež WO₃ v TiO₂-WO₃ kompozitnem filmu, se to nanaša tudi na odvisnost med mehanskimi lastnostmi in lastnostmi strukture. Dobljeni rezultati kažejo, da sta H_{IT} in E_{IT} močno odvisna od koncentracije nanešenega WO₃. Določene vrednosti H_{IT} in E_{IT} se opazno zmanjšajo (v primerjavi z H_{IT} in E_{IT} plasti iz čistega (100 %) TiO₂) ko se nanese WO₃ z nizko koncentracijo (do 2,5 % delež W). Pri nanosih WO₃ z višjo koncentracijo (nad 2,5 % delež W), vrednosti H_{IT} in E_{IT} naraščata skoraj linearno z povečevanjem deleža WO₃ v osnovi. Opaženo neproporcionalno obnašanje H_{IT} in E_{IT} je povezano s specifičnimi spremembami v strukturi in z razvojem napak v nanešeni TiO₂-WO₃ kompozitni fazi, kot tudi s povečanjem količine nastale WO₃ faze (pri povečevanju WO₃ (H₂W₃O₁₂) v delovni raztopini), ki jo obkrožajo posamezni TiO₂ delci.

Ključne besede: neorganske spojine, kemijska sinteza, elektronska mikroskopija, elastične lastnosti

1 INTRODUCTION

The multi-functionality of titanium dioxide is of great interest for both contemporary science and technology.¹ It is the most widely used metal oxide for environmental applications², paints, electronic devices³, gas sensors⁴ and solar cells.⁵ Due to the broad range of applications and the importance of nano-sized titanium a large number of preparative methods for its synthesis have been reported, including: high-temperature processes⁶, sol-gel techniques⁷, chemical vapor deposition⁸, solvothermal processes⁹, reverse micelles¹⁰, hydrothermal methods¹¹, ball milling¹², plasma evaporation¹³, sonochemical reactions¹⁴, etc. Unlike many other techniques, spray pyrolysis represents a simple and cost-effective processing

method, which employs precursor solutions to form different types of dense or porous mono- and multiphase layers with a wide range of thicknesses. This method is also extremely versatile due to the large number of adjustable process parameters such as: substrate temperature, composition and concentration of the precursor, atomization technique, spray geometry, liquid- and gas-flow rates, etc.¹⁵

In this regard, extensive research has been carried out over the past few decades for characterizing the chemical, physical-chemical and surface/bulk-structural properties of these layers synthesized by spray-pyrolysis.^{16–22} However, investigations of their mechanical properties (such as microhardness and indentation hardness, wear resistance, indentation modulus, adhesion,

cohesion, etc.) which are very important in functional and operation exploitation aspects are practically absent.

As a very important addition it has to be pointed out that the anatase nanocrystalline form of titanium dioxide is of particular interest, because it has the highest reactivity in photocatalysis and the best antimicrobial activity.^{23–27} However, there is still a problem with the ability of TiO₂ to respond only to a small portion of the solar spectrum (<5 %) due to its relatively wide band gap (~3.2 eV).²⁸ This invokes the necessity to create a new generation of nano-sized photocatalysts based on TiO₂, being capable of utilising effectively both components (UV and visible) of the sunlight.^{29,30} It is established that doping TiO₂ with different metals or nonmetals (such as SnO₂³¹, WO₃³², ZrO₂³³ and V₂O₅³⁴) is a modification approach, used to extend the absorption range of TiO₂ to the visible region of solar light. The different dopant ions introduce electron energy levels narrowing the TiO₂ band gap. In this aspect the TiO₂-WO₃ composite material^{35,36} seems promising for visible-region-induced photocatalysis, due to the suitable combination of the energy band gaps for anatase and for WO₃. That is why several investigations were focused on the synthesis and characterization of TiO₂-WO₃ composites.^{37–41} The energy band gap of WO₃ is ~2.4–2.8 eV and both the upper edge of the valence band and the lower edge of the conduction band of WO₃ are lower than those of TiO₂. Thus, the TiO₂-WO₃ composite has a narrower energy band gap (compared to that of TiO₂) and shows enhanced photocatalytic activity with respect to its single components. This coupling of TiO₂ and WO₃ favors the transition of electrons from the valence to the conduction band and hole transfers between the bands in the opposite direction. This also reduces the electron-hole recombination rate in both semiconductors.⁴²

It was also recently shown that the unique optical and electric properties of TiO₂ unveil the possibility for its use also as photo-catalytic anticorrosion protection of steels.^{43–49} Considering the investigation of T. Tsai and co-authors⁵⁰ it is expected that deposited on steel, TiO₂ layers will create photocathode protection under the influence of UV irradiation. This protection property is based on the transfer of photo-generated electrons to the metal substrate, as a result of which its electrode potential becomes more electronegative than its corrosion potential. Consequently, the titanium oxide (in the system TiO₂/steel) will act as a non-soluble anode, providing cathode protection of the steel. Obviously, the protective layer of pure TiO₂ cannot act as photo-generated cathodic protector in the dark. However, it can be expected that doping TiO₂ with WO₃, SnO₂, MoO₃, etc., could solve this problem. These semiconductors (WO₃, SnO₂, MoO₃, etc.), which are characterized with a different energy level from those of TiO₂, can store excess electrons during UV irradiation and the stored electrons can be later released in the dark period of the corrosion attack.

Going back to the considered TiO₂-WO₃ system here, it should be pointed out that the methods of preparation of TiO₂-WO₃ systems and the characterization of their catalytic and physicochemical properties are extensively studied and discussed in the literature. Nevertheless, the data for their physical-mechanical properties are very few. Generally, the available data is obtained indirectly using the reference data of chemically or metallurgically synthesized powders that may not be proper for a determination of the properties of the materials deposited as layers/coatings (by other methods) on a specific substrate like metal, alloy, ceramics, etc.⁵¹ And to the best of our knowledge, there are no studies of thin layers obtained by spray-pyrolysis on foreign substrates. For this reason, it is essential to perform studies characterizing the mechanical properties of TiO₂, WO₃, as well as of layers composed of TiO₂-WO₃ mixtures. A knowledge about the mechanical properties is important from the exploitation point of view. The layers of TiO₂, WO₃, and TiO₂-WO₃ mixtures are exposed to a wide range of static and dynamical mechanical loads, temperature variations as well as corrosion, and other factors that lead to the degradation of their strength characteristics.⁵² The interaction of the layers with the substrate should also be investigated. Exceptionally, it is important to consider the formation of composite TiO₂-WO₃ layers on a steel substrate by spray-pyrolysis, because the process is taking place at high temperatures and it is possible to have chemical or structural interactions in the volume of the layer, as well as diffusion transitions on the TiO₂-WO₃/Substrate interface. Therefore, it is highly likely that the mechanical properties of the layer and those of the interface may differ significantly.

The objective of this investigation was to determine the indentation hardness (H_{IT}) and indentation modulus (E_{IT}) of the layers of TiO₂ and WO₃ deposited by spray-pyrolysis on stainless steel (OC 404), as well as to study the influence of the process parameter concentration of the co-deposited WO₃ in the mixed TiO₂-WO₃ layers. Since H_{IT} and E_{IT} are properties that depend on the structure, the structural and morphological changes and phase-chemical content/composition of the layers were carefully investigated, especially with regard to the increase in the WO₃ content (from 1 % to 75 % of mass fractions) in the working solution and in the deposited composite TiO₂-WO₃ layers, respectively.

2 THEORETICAL ASPECTS OF NANO-INDENTATION AS A METHOD FOR THE MECHANICAL CHARACTERIZATION OF THIN FILMS

Instrumented-indentation testing (IIT or so-called nano-indentation) has been developed over the past decade for the purpose of probing the mechanical properties of very small volumes.^{53–57} IIT is ideal for mechanically characterizing thin films, coatings, and surface layers. In addition IIT is an attractive method to

characterize the mechanical properties, because in most cases it requires little sample preparation efforts and has high measurement precision.

Basically, IIT uses a high-resolution actuator to control the penetration into the test surface by the indenter and a high-resolution sensor to continuously measure the penetration depth. One of the benefits of this method is that the contact area under load can be calculated in most cases from the load-displacement data alone, meaning that the residual impression does not have to be viewed directly using complicated imaging techniques, thus making it far easier to measure properties on the sub-micron scale. Indentation hardness (H_{IT}) and indentation modulus (E_{IT}) are the properties most frequently determined by IIT.⁵⁸

The fundamental relation from which the elastic modulus E_{IT} can be estimated is the well-known relation between the true projected contact area A_c , the initial unloading slope S and the reduced elastic modulus E_r .^{59,53}

$$E_r = \frac{\sqrt{\pi}}{2\beta} \frac{S}{\sqrt{A_c}} \quad (1)$$

where β is a constant that depends on the geometry of the indenter tip. For indenters with a triangular cross-section like the Berkovich tip $\beta = 1.034$. The true projected area is determined using the true contact depth h_c and employing the approximation given below with coefficients obtained after calibration using indentation data from a standard fused-silica sample:

$$A_c \approx C_0 h_c^2 + C_1 h_c + C_2 h_c^{1/2} + C_3 h_c^{1/4} + C_4 h_c^{1/8} + C_5 h_c^{1/16}$$

The indentation hardness is defined through the ratio of the applied load P and the corresponding true projected contact area:

$$H_{IT} = \frac{P}{A_c} \quad (2)$$

The indentation (elastic) modulus E_{IT} of the test material is calculated using the relation:

$$E_{IT} = (1-\nu^2) \left[\frac{1}{E_r} - \frac{1-\nu_i^2}{E_i} \right]^{-1} \quad (3)$$

where ν is the Poisson's ratio for the test material, and E_i and ν_i are the indenter's elastic modulus and Poisson's ratio, respectively.⁵⁴ In our case we used the elastic constants for diamond $E_i = 1141$ GPa and $\nu_i = 0.07$.

3 EXPERIMENTAL PART

3.1 Preparation of the samples

The spray-pyrolysis method has been applied for the synthesis of TiO₂-WO₃ composite coatings on foils of Sandvik OC 404 stainless steel (SS). A homemade spray-pyrolysis apparatus for the synthesis of these composites is presented in previously published studies.⁶⁰ As

precursors, a 0.02-M TiO₂ colloidal solution and 0.02-M H₂W₃O₁₂ were used. A colloidal solution containing TiO₂ nanoparticles ($d \approx 4.5$ nm) was synthesized in the manner previously described by T. Rajh et al.⁶¹ A solution of H₂W₃O₁₂ was prepared by dissolving the metal W in H₂O₂ at 60 °C. These two precursor solutions are mixed in different weight ratios in order to vary the contents of WO₃ and TiO₂ in the composites. The stainless-steel specimens (foil thickness 35 μm, 1.5 cm × 10 cm), prior to depositions of the oxide layer, were subjected to standard procedures of degreasing and ultrasonic cleaning.

The typical twin-fluid spray pyrolysis system, using a nozzle made of Pyrex glass, diameter of 0.2 mm, was applied within a homemade computer-controlled device that enabled nozzle movement with adjustable speed and direction. The key preparation parameters of the synthesized samples are presented in **Table 1**.

Table 1: Key preparation parameters of spray pyrolysis

Tabela 1: Ključni parametri pri pršilni pirolizi

Initial temperature of substrate (°C)	460
Nozzle to substrate distance (cm)	4
Nozzle speed (mm/s)	1
Diameter of spraying spot on the substrate (cm)	2
Concentration in precursor solutions (M)	0.02 (TiO ₂ colloidal solution) 0.02 (H ₂ W ₃ O ₁₂)
Air-flow rate (L/h)	300
Precursor solution flow rate (mL/h)	44
Number of nozzle passes	200
Duration of spraying (min)	50

The synthesized samples were named: TiO₂(100), TiO₂(99)-WO₃(1), TiO₂(95)-WO₃(5), TiO₂(90)-WO₃(10), TiO₂(75)-WO₃(25), TiO₂(50)-WO₃(50), TiO₂(25)-WO₃(75), and WO₃(100), according to the content (w/%) of single component in the working solution.

The thicknesses of the coatings were determined according to the relation in Equation (4):

$$T = \frac{M}{A\rho} \quad (4)$$

where A is the geometric area of the coated surface, the mass (M) and the bulk density (ρ) of the coatings. The mass of the coating (M) was determined by weighing the foil before and after the spray pyrolysis.

The coating bulk density is calculated according to Equation (5) and using the true density of anatase ($\rho_A = 3.9$ g/cm³) and WO₃ phase ($\rho_B = 5.4$ g/cm³), the percentage of anatase (k_A) and WO₃ phase (k_B) in the precursor solution, and the powder sample porosity (P) obtained by mercury intrusion porosimetry:⁶²

$$\rho = (\rho_A k_A + \rho_B k_B)(1-P) \quad (5)$$

Although the characteristics of these powders were not entirely the same as that of the films, the porosity of these powders should be considered valuable for an evaluation of the properties of pure TiO₂ and WO₃ coatings as well as of TiO₂-WO₃ composites, such as bulk density, thickness and surface area.

3.2 Structural characterization

The surface morphology, structure and elemental microanalysis of the samples were characterized by scanning electron microscopy (SEM) using a JEOL JSM 6390 electron microscope (Japan) equipped with an ultra-high-resolution scanning system in a regime of secondary-electron image (SEI), back-scattered electrons (BEI) and an INCA energy-dispersive X-ray spectrometer (EDS). The accelerating voltage was 25 kV, I ~ 65 mA. The vacuum was 10⁻⁶ mm Hg.

3.3 Mechanical characterization

The indentation modulus E_{IT} and hardness H_{IT} of the deposited TiO₂, composite TiO₂-WO₃ and WO₃ films were determined via the instrumented indentation technique. The tests were performed using NanoIndenter G200 (Agilent Technologies) equipped with a Berkovich three-sided diamond pyramid with centerline-to-face angle of 65.3° and a 20 nm radius at the tip.⁶³

The particular indentation method employed here is described in ⁶⁴. It prescribes a series of 10 loading/unloading cycles in a single-indentation experiment. The maximum prescribed load is 0.49 N with 20 s peak hold time at the maximum load for each loading-unloading cycle. As a result of the nano-indentation experiments, load-displacement curves are obtained and H_{IT} and E_{IT} are calculated as explained above using the Oliver & Pharr approximation method⁵³ and Equations 1 to 3. Within this study the indentation hardness and modulus were determined using the stiffness calculated by employing 50 % of the upper portion of the load-displacement curve during each unloading cycle. Each sample

Table 2: Estimated surface area, bulk density and thickness of TiO₂-WO₃ samples

Tabela 2: Površina, gostota in debelina vzorcev TiO₂-WO₃

Sample	Deposited mass, mg	Specific surface area, m ² /g	Bulk density, g/cm ³	Thickness, μm
TiO ₂ (100)	3.25	32.3 (5)*	2.27	0.95 (5.8)**
TiO ₂ (99)-WO ₃ (1)	3.40	32.1 (6)	2.30	0.98 (5.6)
TiO ₂ (95)-WO ₃ (5)	3.90	31.1 (7)	2.42	1.07 (5.1)
TiO ₂ (90)-WO ₃ (10)	4.05	30.0 (7)	2.58	1.04 (5.3)
TiO ₂ (75)-WO ₃ (25)	4.80	26.7 (8)	3.04	1.05 (5.2)
TiO ₂ (50)-WO ₃ (50)	5.15	21.1 (10)	3.81	0.90 (6.1)
TiO ₂ (25)-WO ₃ (75)	7.05	15.5 (12)	4.58	1.02 (5.4)
WO ₃ (100)	8.10	9.9 (15)	5.36	1.01 (5.4)

*Standard deviation of specific surface area (%)

**Standard deviation of thickness (%)

was subject to 25 indentation tests in order to have better statistics.

For the realization of an adequate and correct assessment of the mechanical properties of the considered thin deposited layers, it is necessary to guarantee a very good adhesion of the layers to the substrate, reduce the uncertainty in the determination of the layer thickness as well as to have a previous knowledge about the material's internal structure and the existing defects in the layers. The quality of the adhesion of the coatings deposited on the SS substrate was examined by observing whether there is a detachment of the coating from the substrate after a repeated bending of the foil at angle of 180° (EN ISO 2819-1994:2.9 "Bending test").

4 RESULTS AND DISCUSSION

4.1 Analytical and structural characterization of the specimens

The coatings' thicknesses, calculated according to Equation (4), are about 1 μm for all the samples, as presented in **Table 2**.

More details about the porous structure for pure TiO₂ and WO₃ powders, which are constituent parts of all the composites, are given in ⁶².

XRD data obtained for the same systems in our previous investigation confirm the formation of only the anatase phase of TiO₂, no reflections corresponding to the rutile TiO₂ phase were observed.⁶² The composites with WO₃ content greater than 10 % of mass fractions exhibits diffraction peaks of monoclinic tungsten oxide. The absence of reflections corresponding to WO₃ for samples with WO₃ content below 10 % of mass fractions reveals that clusters of WO₃ are present either in the highly dispersed form or in a concentration below the detection limit of the XRD apparatus.

For confirmation of the presence of WO₃ in the layers deposited from the working solutions with a WO₃ content below 10 % of mass fractions, which may not be detected by XRD analysis, we realized the investigation of all the TiO₂-WO₃ composite layers by EDX analysis for sufficient time of exposure (120 s). The results from the EDX analysis are shown in **Tables 3** and **4**.

Table 3: Estimated by EDX analysis percent concentration (at%) of O, Ti and W in deposited by spray-pyrolysis thin TiO₂-WO₃ layers

Tabela 3: EDX-koncentracija (at%) O, Ti in W v tankih TiO₂-WO₃ plasteh, nanešenih s pršilno pirolizo

Sample	O at%	Ti at%	W at%	Total
100 % TiO ₂	80.44	19.56	0	100
TiO ₂ (99)-WO ₃ (1)	81.16	18.22	0.62	100
TiO ₂ (95)-WO ₃ (5)	70.83	27.37	1.80	100
TiO ₂ (90)-WO ₃ (10)	77.57	20.04	2.39	100
TiO ₂ (75)-WO ₃ (25)	72.95	20.89	6.16	100
TiO ₂ (50)-WO ₃ (50)	79.47	10.07	9.83	100
TiO ₂ (25)-WO ₃ (75)	76.83	6.33	16.84	100
100 % WO ₃	76.41	0	23.59	100

Table 4: Estimated by EDX analysis percent concentration (w/%) of O, Ti and W in deposited by spray-pyrolysis thin TiO₂-WO₃ layers**Tabela 4:** EDX-koncentracija (w/%) O, Ti in W v tankih TiO₂-WO₃ plasteh, nanešenih s pršilno pirolizo

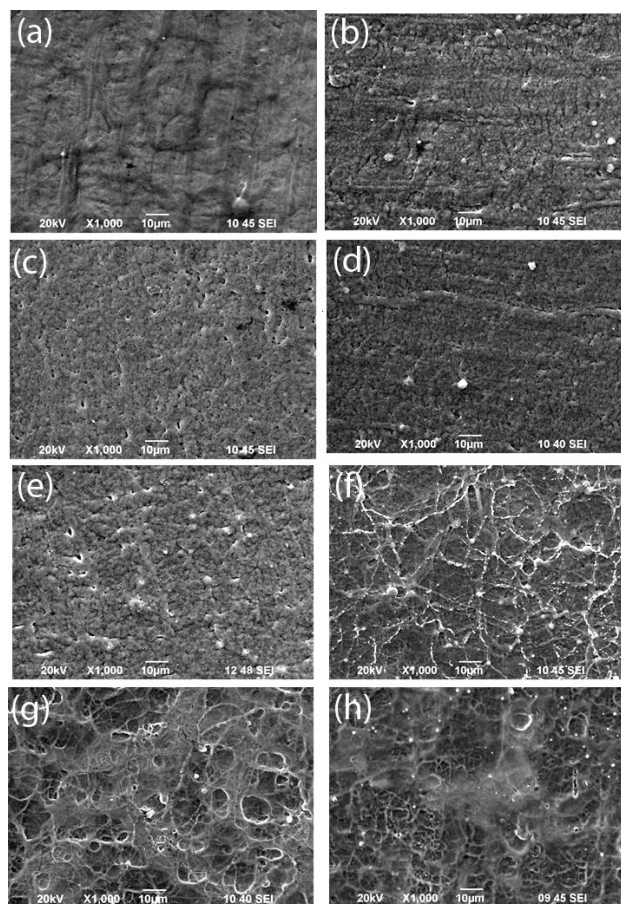
Sample	O w/%	Ti w/%	W w/%	Total
TiO ₂ (100)	57.86	42.14	0	100
TiO ₂ (99)-WO ₃ (1)	56.85	38.21	4.94	100
TiO ₂ (95)-WO ₃ (5)	40.83	47.23	11.94	100
TiO ₂ (90)-WO ₃ (10)	47.00	36.35	16.65	100
TiO ₂ (75)-WO ₃ (25)	35.36	30.32	34.32	100
TiO ₂ (50)-WO ₃ (50)	35.40	14.27	50.33	100
TiO ₂ (25)-WO ₃ (75)	26.56	6.55	66.89	100
WO ₃ (100)	21.99	0	78.01	100

It is seen from the obtained results, that at concentrations of WO₃ in the precursor lower than 10 %, its inclusion in the composite layers takes place. At the same time the content of co-deposited WO₃ and TiO₂ in the composite TiO₂-WO₃ thin films practically does not

correspond to the weight ratio of the two mixed precursor solutions (**Tables 3 and 4**). A specific deviation is observed, especially at the concentration interval of 1–10 % of mass fractions of WO₃ in the working solution. It is interesting to point that for the solution containing 5 % WO₃ both the weight and atomic percentages of co-deposited Ti are having their maximum along all the investigated samples and are even higher than in the case of the spray-pyrolysis deposited pure TiO₂, while the atomic percent of O has its minimum in this case.

The results of the SEM observations of the investigated TiO₂-WO₃ composite layers as well as pure TiO₂ and WO₃ layers at different magnifications are shown in **Figure 1**. It is seen from the obtained results that the surface structure of the pure TiO₂ layer is very smooth and compact, with no visible cracks (**Figure 1a**). The addition of WO₃ (H₂W₃O₁₂) to the working solution affected the structure of the obtained TiO₂-WO₃ composites and the layer surface morphology becomes well populated with irregularities, which can be associated with the irregular inclusion of WO₃ particles into the TiO₂ matrix (**Figures 1b to 1g**). At the low concentrations of WO₃ in the working solution there is a systematic appearance of macro-void formations. With increasing the content of WO₃ in the working solution and the content of the WO₃ in the composite layers, respectively, the number of elevations and depressions on the surface increases while the number of formed voids decreases. The surface of the composite coatings becomes lacy. Probably, this effect is due to the fast hydrolysis of the tungsten salts leaving holes behind them that create micron-sized concavities characterizing the "pure" WO₃ layers (**Figure 1h**). These results are fully consistent with the quantitative analysis of the surface topography and surface roughness obtained for the same systems using AFM.⁶²

As shown in **Figure 1**, the surfaces of the composite layers are decorated by agglomerated grains having a considerable surface roughness. Increasing the content of WO₃ in the TiO₂-WO₃ composites leads to the formation of numerous irregularities in their surface. The layers with a higher WO₃ content exhibit a rough surface texture with high 'mountains' and deep 'valleys' generated by the fusion of particles at the inter-particle contacts. As shown in⁶² there are differences in surface irregularity when forming the TiO₂-WO₃ composites. The surface roughness values increase significantly with an increase of the WO₃ content in the composite, reaching to 316 nm. The change of the surface roughness suggests that the small TiO₂ grains (with average diameter of about 4.5 nm) fill the voids and pores between the WO₃ agglomerates, promoting the surface flattening.

**Figure 1:** SEI images of samples: a) TiO₂(100), b) TiO₂(99)-WO₃(1), c) TiO₂(95)-WO₃(5), d) TiO₂(90)-WO₃(10), e) TiO₂(75)-WO₃(25), f) TiO₂(50)-WO₃(50), g) TiO₂(25)-WO₃(75), and h) WO₃(100).

Slika 1: SEI-posnetki vzorcev: a) TiO₂(100), b) TiO₂(99)-WO₃(1), c) TiO₂(95)-WO₃(5), d) TiO₂(90)-WO₃(10), e) TiO₂(75)-WO₃(25) (eII BEC posnetek), f) TiO₂(50)-WO₃(50) (fI in fIV – BEC posnetek; fIII: EDS-spekter in izračunane vrednosti v spodnji tabeli – Ti in W, dobljena v točki 3 – prikazani na Sliki 1 fII), g) TiO₂(25)-WO₃(75), in h) WO₃(100)

4.2 Mechanical characterization

In order to confirm the high adhesion of the formed coatings we performed adhesion tests with repeated

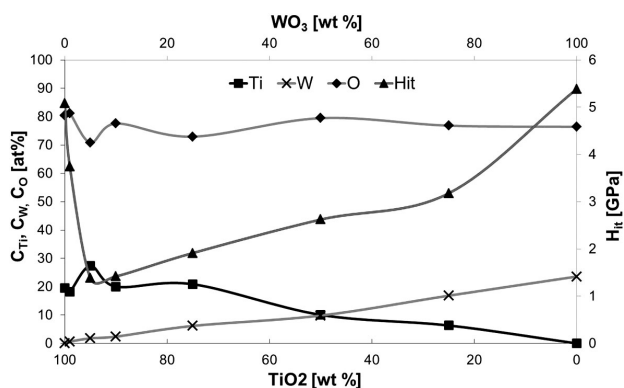
S. CHERNEVA et al.: NANO-INDENTATION INVESTIGATIONS OF THE MECHANICAL PROPERTIES OF THIN TiO_2 , WO_3 ...


Figure 2: Indentation hardness H_{IT} as a function of the concentration of Ti, W and O in the spray-pyrolysis-deposited TiO_2 - WO_3 layers, (at%)

Slika 2: Trdota vtiska H_{IT} v odvisnosti od koncentracije Ti, W in O v plasteh TiO_2 - WO_3 , nanešenih s pršilno pirolizo, (at%)

bending of coated foils at an angle of 180° (according EN ISO 2819-1994:2.9 "Bending test"). A good adhesion of the TiO_2 - WO_3 coatings to the SS substrate was found for all samples, and the attrition of coatings was negligible (less than 1 %). This observation ensures that during the indentation tests there is no separation of the coating from the substrate. This result gives us confidence in excluding the separation of the coating from the analysis of the mechanical properties.

As a result of the nano-indentation measurements, the load-displacement curves for all samples were obtained and analysed for a determination of the indentation modulus and hardness of just the foil coatings. **Figures 2 to 5** present the results from calculated indentation hardness and indentation modulus for all the eight samples at a load of approximately 1.89 mN and indentation depths below 250 nm (25 % of the average film thickness).

The two main factors that may influence the H_{IT} and E_{IT} of the analysed composite thin films are their chemical content and their surface morphology and structure. As shown in **Figure 1** as well as in **Tables 3** and **4**,

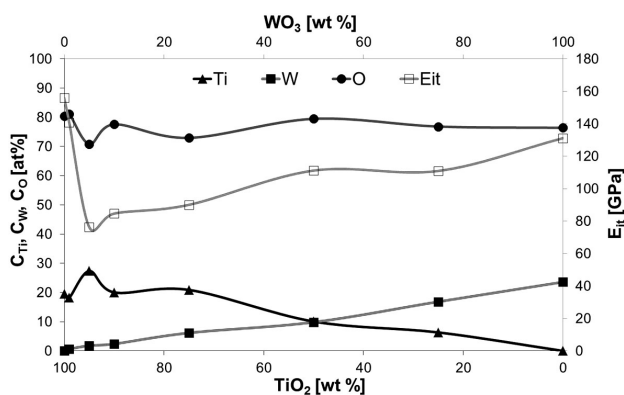


Figure 3: Indentation modulus E_{IT} as a function of the concentration of Ti, W and O in the spray-pyrolysis-deposited TiO_2 - WO_3 layers, (at%)

Slika 3: Modul vtiska E_{IT} v odvisnosti od koncentracije Ti, W in O v plasteh TiO_2 - WO_3 nanešenih s pršilno pirolizo, (at%)

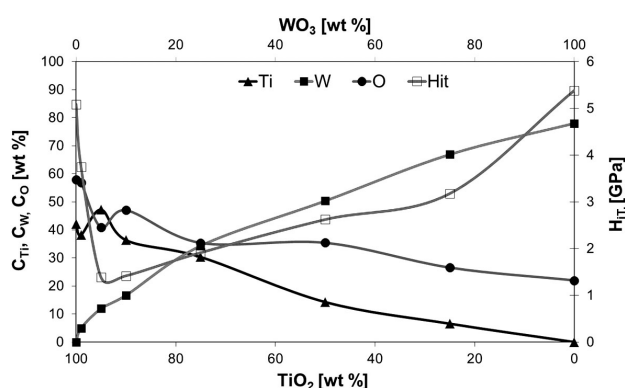


Figure 4: Indentation hardness H_{IT} as a function of Ti, W, and O content, (wt%)

Slika 4: Trdota vtiska H_{IT} v odvisnosti od vsebnosti Ti, W in O, (wt%)

the changes of the chemical content (the ratio between concentrations of TiO_2 and WO_3 phases) in the TiO_2 - WO_3 composite layer have a significant influence on the surface morphology, bulk structure, defects and porosity. This observation suggests that the change in the ratio between the concentrations of the two components and of their ingredients (O Ti, W) in the composite layer could have an important influence on the H_{IT} and E_{IT} values. This was the reason to investigate the influence of the change in the chemical content and the subsequent structural and phase changes in the spray-pyrolysis deposited TiO_2 - WO_3 layer on its mechanical characteristics.

First we consider the variation of the mechanical properties depending on the weight percent of the two precursors in the working solution. **Figures 2** and **4** show that the indentation hardness of the pure WO_3 and pure TiO_2 films is approximately of the same value. The slightly higher hardness of the pure WO_3 coating may be attributed to the observed less porosity. At small concentrations of WO_3 in the working solution (from 0 % to 5 %), there is a rapid drop in the indentation hardness of the obtained composite films. With a further increase of the WO_3 concentrations, the indentation hardness increases gradually to reach its maximum for the pure WO_3 layer. The behaviour of the indentation modulus is

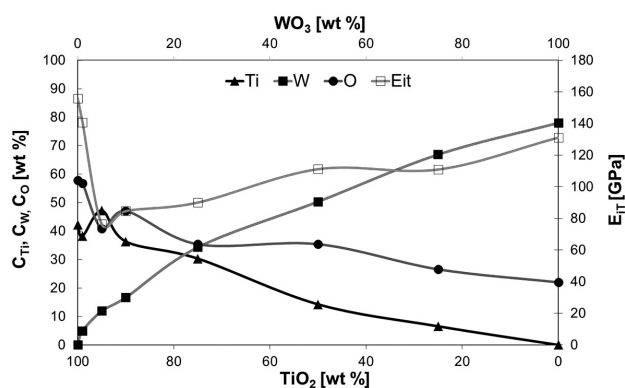


Figure 5: Indentation modulus E_{IT} as a function of Ti, W, and O content, (wt%)

Slika 5: Modul vtiska E_{IT} v odvisnosti od vsebnosti Ti, W in O, (wt%)

Table 5: Values of H_{IT} and E_{IT} at the characteristic points of the concentration ratio of TiO₂ and WO₃ precursors in the working solution, content of Ti and W in deposited layers, respectively**Tabela 5:** Vrednosti H_{IT} in E_{IT} pri značilnih točkah razmerja koncentracije TiO₂ in WO₃ osnov v delovni raztopini ter vsebnost Ti in W v nanješnih plasteh

Weight ratio of the TiO ₂ and WO ₃ precursors in the working solution	TiO ₂ 100 %	TiO ₂ 95 % WO ₃ 5 %	TiO ₂ 50 % WO ₃ 50 %	WO ₃ 100 %
Content (at%) of Ti and W in spray-pyrolysis deposited layers	Ti 19.56 W 0	Ti 27.37 (max) W 1.8 O 70.83 (min)	Ti 10.07 W 9.83 (approx. equal)	Ti 0 W 23.59
H_{IT} (GPa)	5.1	1.3 (min value)	2.7	5.4 (max value)
Standard deviation of H_{IT} (%)	7.8 %	11.99 %	16.68 %	16.3 %
E_{IT} (GPa)	155 (max value)	75 (min value)	110	133
Standard deviation of E_{IT} (%)	4.34 %	7.17 %	9.31 %	9.54 %

similar to that of the indentation hardness. When adding a small amount of WO₃ (from 0 % to 5 %) to the working solution, the indentation modulus of the composite films first decreases with increasing the content of WO₃ and reaches its minimum for sample TiO₂(95)-WO₃(5). With further increasing the concentrations of WO₃, the value of the indentation modulus increases gradually. However, in the case of pure WO₃ film the value of the indentation modulus is less than in the case of pure TiO₂ film.

The relation between the change of H_{IT} and E_{IT} and the chemical content of the investigated layers is also depicted in **Figures 2 to 5**. The results show that the H_{IT} and E_{IT} values of the TiO₂-WO₃ composite layer containing the maximum weight and atomic percent of Ti and minimum atomic percent of O are having the lowest values, as compared to those of the other composite as well as mono-component layers. In this case, the value of H_{IT} was four times lower in comparison with the hardness of the pure TiO₂ layer ($H_{IT}/TiO_2(100)$ 5.1 GPa vs. $H_{IT}/TiO_2(95)-WO_3(5)$ 1.3 GPa). It should be pointed out that the determined concentration of Ti in the deposited composite layer has its maximum value for sample TiO₂(95)-WO₃(5), even higher than the one determined for the spray-pyrolysis deposited nanosize 100 % ("pure") TiO₂ layer (27.4 % of amount fractions vs. 19.6 % of amount fractions of Ti). A remarkable property of the TiO₂(95)-WO₃(5) sample is observed from the Raman spectrum and is discussed in ⁶³. The conclusion is that the Raman spectra of the TiO₂(95)-WO₃(5) sample suggests the appearance of a tensile stress at the TiO₂-WO₃ interface. Such a tensile stress may decrease the hardness of the coating. In our case, the further increase of W percent concentration in the composite coatings has led to a practically proportional increase of H_{IT} . At higher concentrations (above 17 % of amount fractions) the increase of the H_{IT} value became more rapid.

When comparing the variation of H_{IT} with that of the Ti, W and O atomic concentrations in the studied layers, it can be concluded that the increase of the W concentration in the composite layer is monotonic, while that of Ti possesses a complex non-monotonic behaviour. With

the addition of WO₃ into the working solution, first the concentration of the Ti increases, reaching its maximum for TiO₂(95)-WO₃(5) sample. In the case of the working solution containing 10 % WO₃ precursor, the concentration of Ti in the deposited composite TiO₂-WO₃ layer starts to decrease, reaching ~11 % of amount fractions. Increasing the concentration of the WO₃ precursor (up to 25 %) leads to an increase of the concentration of W in the composite layers; however, this does not change proportionally the concentration of Ti. Furthermore, the values of H_{IT} continue to increase, indicating the dominant influence of the second component (WO₃) in the composite layer mechanical characteristics. This is also indicated by the values of H_{IT} at the approximately equal atomic concentration ratio of Ti and W – **Table 5**.

The values of H_{IT} and E_{IT} for the spray-pyrolysis deposited layers of TiO₂, WO₃ and TiO₂-WO₃ composites with weight ratio of the TiO₂ and WO₃ precursors 95:5 and 50:50 corresponding respectively to maximum concentration of Ti (27.5 % of amount fractions) and minimum concentration of O (70.83 % of amount fractions) and to the approximately the same content in % of the amount fractions of Ti and W (10.07:9.83 % of amount fractions) can be found in **Table 5**.

Considering the results discussed above, it can be concluded that the mechanical characteristics H_{IT} and E_{IT} mainly depend on the chemical content, structure and porosity of the investigated TiO₂-WO₃ composite layers. The comparison of the size changes in agglomerates building the layers shows that the amorphous "pure" TiO₂ layers (**Figure 2a**) are characterized by considerably higher H_{IT} and E_{IT} values than those of the composite TiO₂-WO₃ layers. The co-deposition of 0.6–2.4 % of amount fractions (5–17 % of mass fractions) W leads to a substantial increase of the porosity and the size of the agglomerates building the TiO₂-WO₃ layers that determine the dramatic decrease of H_{IT} and E_{IT} , according to the Hall-Petch relationship.⁶⁵ Increasing the concentration of the co-deposited W (WO₃) further, decreases the porosity of the layers, as well as the size of the agglomerates that build them, which leads to the increase of H_{IT} and E_{IT} .⁶² The latter values are close to the H_{IT} and E_{IT} measured for the spray-pyrolysis

deposited "pure" WO₃, which according to the SEM microphotographs is more likely to exhibit a crystal structure. Importantly, in all of the composite layers the values of H_{IT} and E_{IT} are lower than the one of the "pure" TiO₂ and WO₃ layers. Moreover, the obtained values are described by a dependency that has a minimum at low concentrations (1.5–2.5 % of amount fractions) of the co-deposited W, after which H_{IT} and E_{IT} increase with the concentration of W. This complex dependency suggests that along with the influence of the changes in the structure (the size of the crystallites that build the layers) other factors could have an influence on H_{IT} and E_{IT} when the concentration of co-deposited W (WO₃, respectively) increases in the composite layers. We can assume that the TiO₂ and WO₃ molecules interact in the TiO₂-WO₃ composite layer on an electron level. The reasons for making such an assumption are given in 62,66–68.

4.3 Further discussion

It is interesting to note that H_{IT} and E_{IT} drop coincides with the rise of the photoactivity of the corresponding TiO₂-WO₃ systems.⁶² After reaching the maximum values of the photocatalytic activity at 10 wt. % of WO₃, the drop of activity occurred with further increasing of the WO₃ content. The drop of photoactivity is followed by a simultaneous increase of the H_{IT} and E_{IT} factors. Obviously, materials properties that suits photocatalytic activities (well-developed surface area, porosity, surface defect, etc.) are a disadvantage for the mechanical characteristics of these coatings. Our previous investigations by XPS⁶² have shown that metals are in their main oxidation state, Ti⁴⁺ and W⁶⁺, but positive shift of the binding energy of Ti 2p by 0.5 eV is observed, pointing out that there is kind of interaction between TiO₂ and WO₃ phase. Furthermore, the Raman investigation reveals that TiO₂-WO₃ composites with up to 10 % of mass fractions of WO₃ are without free WO₃ phase that is incorporated within TiO₂ forming Ti_{1-x}W_xO₂ phase. Probably, such a structure leads to the disturbance of TiO₂ lattice, making it less resistant to the mechanical stress. Obviously, this increasing of the quantity of defects in the TiO₂-WO₃ composite phase and the increasing of the quantity of separately formed WO₃ phase (with increasing of WO₃ (H₂W₃O₁₂) in the working solution) surrounded by solitary TiO₂ particles can be another reason that will lead to an increase of the H_{IT} and E_{IT} of the deposited by spray-pyrolysis layers.

5 CONCLUSION

In present work it was shown that the mechanical properties of a deposited spray-pyrolysis composite's TiO₂-WO₃ layers strongly depend on the concentration of WO₃ (weight ratio between the two precursor solutions (TiO₂ colloidal solution and H₂W₃O₁₂), respectively) in the working solutions. For low concentrations

of the WO₃ (up to 10 %) in the working solution, the indentation hardness and modulus of the studied films decrease, due to the increase of the porosity and size of the building agglomerates. However, for higher concentrations of WO₃ (more than 10 %), the increase of H_{IT} and E_{IT} with the increase of the concentration of WO₃ can be attributed to the decrease of the size of the building agglomerates of the phase TiO₂-WO₃, as well as to filling of the concavities and pores between the separate WO₃ agglomerates with small-size TiO₂ grains that flatten the surface of the composite layer. The observed specific changes of H_{IT} and E_{IT} can also be associated with the interaction between the TiO₂ and the WO₃ in the TiO₂-WO₃ composites at the electron level. Moreover, it was found that increasing the defects in the TiO₂-WO₃ composite phase and increasing the quantity of separately formed WO₃ phases (with increasing of WO₃ (H₂W₃O₁₂) in the working solution) surrounded by solitary TiO₂ particles can be another reason leading to increasing of H_{IT} and E_{IT} of the spray-pyrolysis layers.

Acknowledgements

The authors gratefully acknowledge the financial support by the National Science Fund of Bulgaria under Projects: T 02-22 and DNTS/Germany 01/6; and Ministry of Education and Science of the Republic of Serbia – Project No. 172022.

6 REFERENCES

- I. V. Baklanova, V. N. Krasilnikov, L. A. Perelyaeva, O. I. Gyrdasova, *Theoretical and Experimental Chemistry*, 47 (2011), 215–218, doi:10.1007/s11237-011-9206-x
- W. Choi, *Catalysis Surveys from Asia*, 10 (2006), 16–28, doi:10.1007/s10563-006-9000-2
- U. Bach, D. Corr, D. Lupo, F. Pichot, M. Ryan, *Adv. Mater.*, 14 (2002), 845–848, doi:10.1002/1521-4095(20020605)
- P. I. Gouma, M. J. Mills, K. H. Sandhage, *J. Am. Ceram. Soc.*, 83 (2000), 1007–1009, doi:10.1111/j.1151-2916.2000.tb01320.x
- C. C. Oey, A. B. Djurišić, H. Wang., K. K. Y. Man, W. K. Chan, M. H. Xie, Y. H. Leung, A. Pandey, J.-M. Nunzi, P. C. Chui, *Nanotechnology*, 17 (2006), 706–713
- R. N. Grass, S. Tsantilis, S. E. Pratsinis, *AIChE Journal*, 52 (2006), 1318–1325, doi:10.1002/aic.10739
- L. Kao, T. Hsu, H. Lu, *J. Colloid Interf. Sci.*, 316 (2007), 160–167, doi:10.1016/j.jcis.2007.07.062
- X. Zhang, M. Zhou, L. Lei, *Appl. Catal. A- Gen.*, 282 (2005), 285–293, doi:10.1016/j.apcata.2004.12.022
- M. Kang, *Mater. Lett.*, 59 (2005), 3122–3127, doi:10.1016/j.matlet.2005.05.032
- X. Sui, Y. Chu, S. Xing, M. Yu, C. Liu, *Colloid. Surface A.*, 251 (2004), 103–107, doi:10.1016/j.colsurfa.2004.08.015
- K. Mori, K. Maki, S. Kawasaki, S. Yuan, H. Yamashita, *Chem. Eng. Sci.*, 63 (2008), 5066–5070, doi:10.1016/j.ces.2007.06.030
- C. Shifu, C. Lei, G. Shen, C. Gengyu, *Chem. Phys. Lett.*, 413 (2005), 404–409, doi:10.1016/j.cplett.2005.08.038
- T. Miyata, S. Tsukada, T. Minami, *Thin Solid Films*, 496 (2006), 136–140, doi:10.1016/j.tsf.2005.08.294
- W. Guo, Z. Lin, X. Wang, G. Song, *Microelectron. Eng.*, 66 (2003), 95–101, doi:10.1016/S0167-9317(03)00031-5

- ¹⁵ A. B. Haugen, I. Kumakiri, C. Simon, M. A. Einarsrud, J. Eur. Ceram. Soc., 31 (2011), 291–298, doi:10.1016/j.jeurceramsoc.2010.10.006
- ¹⁶ T. Novakovic, N. Radic, B. Grbic, D. Stoychev, P. Stefanov, T. Marinova, Mater. Sci. Forum, 555 (2007), 321–326
- ¹⁷ T. Novakovic, N. Radic, B. Grbic, V. Dondur, M. Mitric, D. Randjelovic, D. Stoychev, P. Stefanov, Appl. Surf. Sci., 255 (2008), 3049–3055, doi:10.1016/j.apsusc.2008.08.074
- ¹⁸ L. M. Bertus, A. Enesca, A. Duta, Thin Solid Films, 520 (2012), 4282–4290, doi:10.1016/j.tsf.2012.02.052
- ¹⁹ O. Sugiyama, M. Okuya, Sh. Koneko, J.Ceramic Soc.Japan, 117 (2009), 203–207, doi.org/10.2109/jcersj2.117.203
- ²⁰ J. M. Ortega, A. Martinez, D. Acosta, C. Magana, Sol. Energ. Mat. Sol., C. 90 (2006), 2471–2479, doi:10.1016/j.solma.2006.10.033
- ²¹ J. Dostanic, B. Grbic, N. Radic, P. Stefanov, Z. Saponjic, J. Buha, Chem. Eng. J., 180 (2012), 57–65, doi:10.1016/j.cej.2011.02.100
- ²² M. Maeda, T. Horikawa, MRS Proceedings (2013), mrsf12-1492-g07-07, doi:10.1557/opl.2013.220
- ²³ A. Fujishima, X. Zhang, D. A. Tryk, Surf. Sci. Rep., 63 (2008), 515–582, doi:10.1016/j.surfrep.2008.10.001
- ²⁴ M. Grätzel, Mod. Aspect. Electrochem., 15 (1983), 83–165
- ²⁵ P.V. Kamat, Chem. Rev., 93 (1993), 267–300, doi:10.1021/cr00017a013
- ²⁶ M. Machida, K. Norimoto, T. Kimura, J. Am. Ceram. Soc., 88 (2005), 95–100, doi:10.1111/j.1551-2916.2004.00006.x
- ²⁷ A. Markowska-Szczupaka, K. Ulfig, A.W. Morawski, Catal. Today, 169 (2011), 249–257, doi:10.1016/j.cattod.2010.11.055
- ²⁸ K. Sridharan, E. Jang, T. J. Park, Appl. Catal. B: Environ., 142–143 (2013), 718–728, doi:10.1016/j.apcatb.2013.05.077
- ²⁹ D. Chatterjee, S. Dasgupta, J. Photoch. Photobio., C 6 (2005), 186–205, doi:10.1016/j.jphotochemrev.2005.09.001
- ³⁰ J. Radjenovic, C. Sirtori, M. Petrovic, D. Barcelo, S. Malato, Appl. Catal. B: Environ., 89 (2009), 255–264, doi:10.1016/j.apcatb.2009.02.013
- ³¹ S. Chen, A. Wang, C. Dai, J. Benziger, Y. Lin, Chem.Eng.J., 249 (2014), 48–53, doi:10.1016/j.cej.2014.03.075
- ³² S. Stojadinovic, N. Radic, R. Vasilic, M. Petkovic, P. Stefanov, Lj. Zekovic, B. Grbic, Appl.Catal. B: Environ., 126 (2012), 334–341, doi:10.1016/j.apcatb.2012.07.031
- ³³ A. Kambur, G. Pozan, I. Boz, Appl.Catal. B, 115–116 (2012), 149–158, doi:10.1016/j.apcatb.2011.12.012
- ³⁴ M. A. Rauf, S. B. Bukallah, A. Hammadi, A. Sulaiman, F. Hammadi, Chem. Eng. J., 129 (2007), 167–172, doi:10.1016/j.cej.2006.10.031
- ³⁵ V. Puddu, R. Mokaya, G. Li Puma, Chem. Commun., 45 (2007), 4749–4751, doi:10.1039/B711559H
- ³⁶ O. Lorret, D. Francova, G. Waldner, N. Stelzer, Appl. Catal. B: Environ., 91 (2009), 39–46, doi:10.1016/j.apcatb.2009.05.005
- ³⁷ R. A. Carcel, I. Andronic, A. Duta, Mater. Charact., 70 (2012), 68–73, doi:10.1016/j.matchar.2012.04.021
- ³⁸ J. Georgieva, S. Armanyanov, E. Valova, Ts. Tsacheva, I. Poullos, J. Electroanal. Chem., 585 (2005), 35–43, doi:10.1016/j.elechem.2005.07.018
- ³⁹ E. Valova, J. Georgieva, S. Armanyanov, S. Sotiropoulos, A. Hubin, K. Baert, M. Raes, ECS Trans., 25 (2010), 13–24, doi:10.1149/13318500
- ⁴⁰ M. Ilieva, S. Ivanov, V. Tsakov, J. Appl. Electrochem., 38 (2008), 63–69, doi:10.1007/s10800-007-9399-9
- ⁴¹ M. Ilieva, A. Nakova, V. Tsakova, J.Appl.Electrochem., 42 (2012), 121–129, doi 10.1007/s10800-011-0378-9
- ⁴² A. Rey, P. Garcia-Munoz, M. D. Hernandez-Alonso, E. Mena, S. Garcia-Rodriguez, F. J. Beltran, Appl. Catal. B, 154–155 (2014), 274–284, doi:10.1016/j.apcatb.2014.02.035
- ⁴³ T. Tsatsuja, T. Tsatsuja, Y. Ohio, S. Satoh, R. Fujisama, Chem. Mater., 13 (2001), 2838–2842, doi:10.1021/cm010024k
- ⁴⁴ P. Nagootrakarwikat, Y. Ohio, R. Fujisawa, Phys.Chem., 5 (2003), 3234–3237
- ⁴⁵ R. Subavi, Electrochem.Comm., 5 (2000), 897–902, doi:10.1016/j.elecomm.2003.08.016
- ⁴⁶ Y. Takochushi, P. Nagootrakarwikat, T. Tsatsuja, Electrochim. Acta, 49 (2004), 2025–2029, doi:10.1016/j.electacta.2003.12.032
- ⁴⁷ R. Subavi, T. Shinohata, K. Mori, J.Electrochem.Soc., 102 (2005), B105–B110, doi:10.1149/1.1856912
- ⁴⁸ R. Subavi, T. Shinohata, K. Mori, Sci.Technol. Adv.Mater., 6 (2006), 501–507, doi:10.1016/j.stam.2005.01.003
- ⁴⁹ S. Li, Q. Wang, T. Chen, Z. Zhou, Y. Wang, J. Fu, Nanoscale Res. Lett., 7 (2012), 227–232, doi:10.1186/1556-276X-7-227
- ⁵⁰ T. Tsai, S. Chang, T. Hsueh, W. Weng, C. Hsue, B. Dai, Nanoscale Res. Lett., 6 (2011), 575–581, doi:10.1186/1556-276X-6-575
- ⁵¹ K. Hashimoto, I. Hiroshi, A. Fujisima, Jpn. J. Appl. Phys., 44 (2005), 8269–8285, doi:10.1143/JJAP.44.8269
- ⁵² B. Gambin, J. Ivanova, G. Nikolova, V. Valeva, In: Proc. 10-th Conference on Dynamical Systems. Theory and Applications, December 7–10 2009, Lodz, Poland, vol. 2, pp. 823–828
- ⁵³ W. Oliver, G. Pharr, J. Mater. Res., 19 (2004), 3–20, doi:10.1557/jmr.2004.19.1.3
- ⁵⁴ W. Oliver, G. Pharr, J. Mater. Res., 7 (1992), 1564–1583, doi:10.1557/jmr.1992.1564
- ⁵⁵ G.M. Pharr, A. Bolshakov, J. Mater. Res., 17 (2002), 2660–2671, doi:10.1557/JMR.2002.0386
- ⁵⁶ J. C. Hay, A. Bolshakov, G. M. Pharr, J. Mater. Res., 14 (1999), 2296–2305, doi:10.1557/JMR.1999.0306
- ⁵⁷ G. M. Pharr, W. C. Oliver, F. R. Brotzen, J. Mater. Res., 7 (1992), 613–617, doi:10.1557/JMR.1992.0613
- ⁵⁸ Agilent Nanoindenter G200 User's Guide, Part Number G2A-13192-1, Rev C, Agilent Technologies, Inc. 2012
- ⁵⁹ G. Pharr, J. Hay, ASM Handbook Volume 08: Mechanical Testing and Evaluation, ASM International. 2008, 231
- ⁶⁰ T. Novakovic, N. Radic, B. Grbic, T. Marinova, P. Stefanov, D. Stoychev, Catal. Commun., 9 (2008), 1111–1118, doi:10.1016/j.cattcom.2007.10.030
- ⁶¹ T. Rajh, A. Ostafin, O. I. Micic, D. M. Tiede, M.C.Thurnauer, J. Phys. Chem., 100 (1996), 4538–4545, doi:10.1021/jp952002p
- ⁶² B. Grbić, N. Radic, S. Stojadinović, R. Vasilic, Z. Dohčević-Mitrović, Z. Šaponjic, P. Stefanov, Surf. Coat. Technol., 258 (2014), 763–771, doi:10.1016/j.surfcoat.2014.07.082
- ⁶³ Agilent Nano Indenter G200 System Pre-Install Information Guide, Agilent Technologies, Inc. 2012
- ⁶⁴ M. Datcheva, S. Cherneva, D. Stoychev, R. Iankov, M. Stoycheva, Mater. Sci. Appl., 2 (2011), 1452–1464, doi:10.4236/msa.2011.210196
- ⁶⁵ W. Smith, J. Hashemi, Foundations of Materials Science and Engineering, 4th ed., McGraw-Hill, New York. 2006
- ⁶⁶ J. Georgieva, E. Valova, S. Armanyanov, N. Philippidis, I. Poullos, S. Sotiropoulos, J. Hazard. Mater., 211–212 (2012), 30–46
- ⁶⁷ C. Khare, K. Sliozberg, R. Meyer, A. Savan, W. Schuhmann, A. Ludwig, Int. J. Hydrogen Energy, 38 (2013), 15954–15964 doi:10.1016/j.ijhydene.2013.09.142
- ⁶⁸ G. Nikolova, Thermomechanical behaviour of thin multi-layered structures, Ph.D. Thesis, Institute of Mechanics – BAS, Sofia, Bulgaria, 2008